J. Fluid Mech. (2003), *vol.* 483, *pp.* 225–248.
DOI: 10.1017/S0022112003004233 Printed in the United Kingdom

Linear and nonlinear instabilities of a Blasius boundary layer perturbed by streamwise vortices. Part 1. Steady streaks

By XUESONG WU[1,2] AND JISHENG LUO[3]

[1]Center for Turbulence Research, Stanford University, CA 94305, USA

[2]Department of Mathematics, Imperial College, 180 Queens Gate, London SW7 2BZ, UK

[3]Department of Mechanics, Tianjin University, China

(Received 28 January 2002 and in revised form 14 January 2003)

This paper investigates the stability properties of a Blasius boundary layer perturbed by a small-amplitude steady three-dimensional distortion, which may be isolated or periodic along the spanwise direction. It is shown that once the strength of the distortion exceeds a threshold, the perturbed flow becomes inviscidly unstable. An isolated distortion which features a dominant low-speed streak induces a localized mode, while a periodic distortion supports spatially quasi-periodic modes through a parametric resonance. The frequencies and growth rates of both types of mode are much higher than those of the viscous Tollmien–Schlichting (T–S) waves. For moderate distortions, the instability modes can be viewed as kinds of modified T–S waves, which amplify at rates in excess of the viscous instability. For a localized distortion, these modes do not reduce to the usual T–S waves in the zero-distortion limit. The nonlinear development of the inviscid modes is also studied, and is found to be governed by a slightly modified version of the evolution equation derived by Wu (1993). A numerical study suggests that nonlinearity has a strong destabilizing effect, and ultimately leads to an explosive growth in the form of a finite-distance singularity. The present theoretical model is found to capture qualitatively some key experimental observations.

1. Introduction

It is well known that the instability of boundary layers is sensitive to their profiles, i.e. a small distortion to the basic flow may have a detrimental effect on its stability. The main interest of the present paper (Part 1) and its sequel (Part 2, Wu & Choudhari 2003) is to investigate the mechanisms by which a relatively weak distortion can significantly affect the instability of an otherwise uniform Blasius flow. Specifically, we shall address two main issues: (*a*) how the Tollmien–Schlichting instability, which operates in the absence of any distortion, is modified by a weak distortion, and (*b*) whether or not a weak distortion is able to cause any inviscid instability.

Many factors can cause three-dimensional steady or unsteady distortions in the form of streamwise (longitudinal) vortices or streaks. These include small steady or unsteady perturbations superimposed on the oncoming flow, imperfections at the leading edge, crossflow instability, Görtler vortices induced by surface curvature as well as certain excitation devices. Distortion of this kind also arises due to the nonlinear interaction between pairs of Tollmien–Schlichting (T–S) waves. The resulting perturbed flows are spanwise-dependent but essentially unidirectional, i.e.

the transverse velocity components are much smaller than the streamwise component. The instability of such transversely sheared flows has attracted a great deal of interest because it appears to be related to various aspects of the transition process, such as secondary instabilities and by-pass transition.

In certain circumstances, the spanwise variation is more or less periodic. For instance, in a boundary layer over a concave surface the Görtler instability drives a secondary flow field of this form. Nayfeh (1981) showed that a resonant interaction occurs between the Görtler vortex system and a pair of oblique T–S waves whose spanwise wavelength is twice that of the Görter vortices. Low-amplitude vortices cause a small modification to the T–S wave growth rate, which he approximated using a multiple-scale method. The effect of vortices with a magnitude comparable with the background Blasius flow was subsequently studied by Nayfeh & Al-Maaitah (1988) using Floquet theory. This work as well as that of Nayfeh (1981) was based on a finite-Reynolds-number formulation. Bennett & Hall (1988) employed high-Reynolds-number approach to analyse the secondary instability of Taylor–Görtler vortices in a curved channel to disturbances on the lower-branch T–S wave scales. The secondary instability on the T–S scales is of course not the only possibility. Depending on the strength and wavelength of the vortices, other possibilities arise. For instance, small-wavelength Görtler vortices as described by Hall & Latkin (1988) support secondary modes that are trapped in the shear layers where the vortices concentrate, as was shown by Hall & Seddougui (1989). The boundary layer perturbed by Görtler vortices with wavelength of the boundary-layer thickness and magnitude comparable with the Blasius flow is unstable to inviscid Rayleigh modes (Hall & Horseman 1991). The last three papers focused on the resonance of fundamental type, for which the spanwise wavelength of the secondary modes equals that of the Görtler vortices.

The resonant interaction of the kind considered by Nayfeh (1981) operates in more general settings. Goldstein & Wundrow (1995) investigated the role of such an interaction for a mean-flow distortion that is generated by imposing a crossflow at a distance L from the leading edge. The spanwise wavelength Λ is taken to be much larger than the boundary-layer width, that is, $\sigma = \Lambda/(R^{-1/2}L) \ll 1$, where R is the Reynolds number based on L. They show that at distances of $O(L\sigma^3)$ from the location of forcing, the perturbed mean flow becomes inflectional for a suitably chosen magnitude of the imposed crossflow. A pair of oblique instability modes with a spanwise wavelength 2Λ may then develop on an inviscid length scale due to their resonance with the distortion. On a purely linear basis, this instability ultimately dies out sufficiently far downstream. However, if the modes attain a threshold magnitude before the final decay, they may interact nonlinearly. Their subsequent development was found to be governed by the amplitude equation derived by Goldstein & Choi (1989) and Wu, Lee & Cowley (1993).

A distortion of particular interest occurs when the boundary layer is subject to a relatively high free-stream turbulence level. As was first observed by Dryden (1936) and Taylor (1939), small low-frequency three-dimensional perturbations in the free stream produce significant distortion within the boundary layer, leading to alternate thickening and thinning of the layer along the spanwise direction. Steady disturbances also cause the same type of variation (Bradshaw 1965). Recent experimental studies show that the distortions are in the form of elongated streaks (see e.g. Kendall 1985 Westin *et al.* 1994 Matsubara & Alfredsson 2001; and references therein). Such streaks are now commonly referred to as Klebanoff modes, as a tribute to the contribution of Klebanoff (1971) (despite the fact that mathematically they are not related to modes of any eigenvalue system). The above-mentioned experiments, along with

those of Blair (1992) and Roach & Brierley (1992), have provided fairly complete quantitative data about the characteristics of Klebanoff modes themselves. However, the instability of the streaks and its role in the transition process remain to be fully understood, though the flow visualization in Matsubara & Alfredsson (2001) provides some important clues. The main obstacle of course is the random nature (in both time and space) of the free-stream disturbances and the associated Klebanoff motion, which make a quantitative study extremely hard. Numerous researchers have instead chosen to investigate the steady distortions that are induced in a controlled manner.

Hamilton & Abernathy (1994) used surface roughness elements to create a single or multiple streamwise vortices. These vortices cause the distorted flow profile to have an inflection point. An inflection point, however, does not always lead to inviscid instability. Only when distortion exceeds a certain critical magnitude do localized inviscid instability waves start to appear. These waves may decay or occasionally develop into turbulent spots if the distortion strength is just above critical. As the distortion is increased further, the local instability leads to persistent self-sustaining turbulent spots.

Asai, Fukuoka & Nishioka (2000) and Asai, Minagawa & Nishioka (2002) investigated in detail the instability of an isolated streak, which was produced by a small screen set normal to the wall. The low-speed streak is shown to support both symmetric (varicose) and antisymmetric (sinuous) modes. These investigators mapped out the amplitude development as well as the spatial structure of each mode. Kogan *et al.* (2001) generated isolated streaks in a boundary layer over a blunt-nosed plate by a thin wire placed upstream and normal to the leading edge. The wake behind the wire has vorticity normal to the wall, and that vorticity is stretched and wraps around the wall surface to form streamwise vortices, a process described by Goldstein, Leib & Cowley (1992) and Ustinov (2001). Kogan *et al.* (2001) carried out detailed measurement of the localized distortion in the boundary layer. The instability of the resulting flow is yet to be studied.

Bakchinov *et al.* (1995) generated periodically distributed longitudinal vortices by arranging roughness-element arrays in a regular spacing along the spanwise direction. The otherwise spanwise-uniform flow was thus modulated in a periodic fashion by these vortices, whose strength was controlled by the roughness height. For strong modulation, inviscid-instability modes were found to develop out of the background disturbances, and their frequencies are well above those of the unstable T–S waves in the undistorted Blasius flow. For moderate modulation, instability waves with typical frequencies of T–S waves can be observed, but they amplify more rapidly than when the distortion is absent.

The artificially created distortions in these experiments are akin to Klebanoff modes. The findings for the former may shed useful light on the instability of the streaks induced by free-stream disturbance. There is evidence to suggest that despite the different origins of the distortions, the instability mechanism of various perturbed flows appears to be somewhat universal. However, it should be noted that the distortions in these experiments are fairly large, being comparable with the mean flow. Therefore caution must be exercised when relating them to the instability of Klebanoff modes, whose magnitude rarely exceeds 10% of the free-stream velocity.

Direct experimental studies of the instability of the Blasius boundary layer in the presence of the Klebanoff modes have been made by a number of investigators. The relevant findings will be reviewed in Part 2.

Obviously, the instability of boundary layers subject to finite-amplitude steady distortions is an interesting and important problem in its own right, and an attack on

it requires a major numerical study. The main concern in the present paper, Part 1, is with the sensitivity of the boundary-layer instability to a steady distortion. For this purpose, it is appropriate to consider the case where the distortion is relatively weak. Such weak distortions are important because they are the ones that are most likely to arise from unavoidable small imperfections in the geometry of both laboratory and actual technological flows. A weak distortion has the advantage of being more amenable to analytical treatment, yet as we shall argue, the resulting simple model may offer relevant insights into the case of stronger distortion.

There have been numerous theoretical studies of the instability of shear flows (boundary layers or channel flows) perturbed by distortions in the form of streaks. The interested reader is referred to a recent paper by Andersson *et al.* (2001) for relevant references. Often the streaks were modelled in a rather *ad hoc* fashion. In the present work, we insist that the distortions must be realizable, at least in principle, i.e. they may be generated either by a certain excitation device or by external disturbances. They must be appropriate (approximate) solutions to the Navier–Stokes equations. To fix the idea, here we consider the instability of the steady distortion that has been considered by Goldstein & Wundrow (1995), while in Part 2 the instability of Blasius boundary layer perturbed by Klebanoff modes will be investigated. The basic observation is that the Blasius profile has a small curvature near the wall, so that even a small distortion may lead to an inflection point and hence to essentially inviscid instabilities.

The essential physical and analytical insights can be gained by an asymptotic approach based on the high-Reynolds-number assumption, which is the only means for providing a self-consistent mathematical description of the key processes involved. In § 2, we formulate the problem in this asymptotic framework, and derive the appropriate scalings. In § 3, the mean-flow distortion induced by imposing a crossflow velocity at a streamwise location is considered. The spanwise distribution of the perturbation is allowed to be either localized or periodic. Since the streamwise location of our interest is farther downstream than that considered by Goldstein & Wundrow (1995), the relevant solution is thus essentially the large-distance limit of the solution given by Goldstein & Wundrow (1995). The linear instability of the perturbed flow is analysed in § 4. It is shown that with a stronger imposed crossflow, instability modes that are different from those identified by Goldstein & Wundrow (1995) may emerge, whether the distortion is periodic or isolated. The relation between the mode identified in this paper and that in Goldstein & Wundrow (1995) will be discussed. The spanwise length scale of these modes is comparable with that of the mean-flow distortion, but their streamwise wavelengths are much shorter. The nonlinear development of the instability modes is investigated in § 5. Finally in § 6, we summarize the results and discuss their implications.

2. Formulation and scalings

Consider the two-dimensional incompressible boundary layer due to a uniform flow U_∞ past a semi-infinite flat plate. As in Goldstein & Wundrow (1995), a small-amplitude spanwise-dependent motion is assumed to be imposed at a distance L downstream from the leading edge of the plate (see figure 1). The Reynolds number is defined as

$$R = U_\infty L/\nu, \tag{2.1}$$

where ν is the kinematic viscosity. We shall assume that $R \gg 1$.

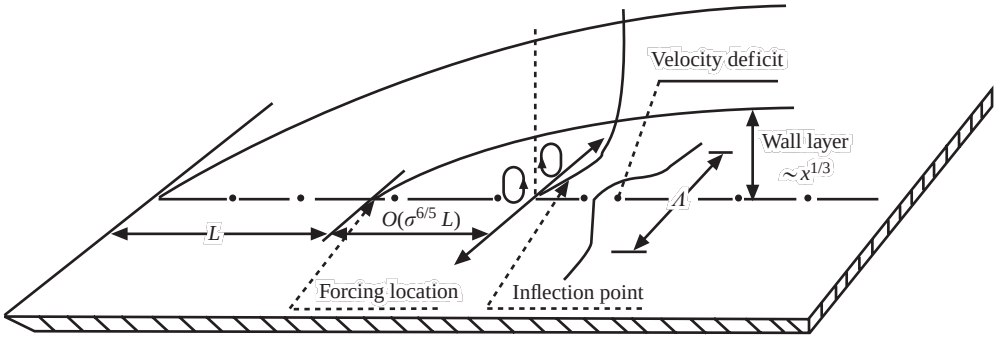

FIGURE 1. A sketch illustrating the problem and relevant scales. A crossflow is imposed at a distance L from the leading edge, generating a pair of counter-rotating streamwise vortices, between which a velocity deficit region forms. An inflection point appears in the wall layer at a distance of $O(\sigma^{6/5}L)$ further downstream, where inviscid instability occurs.

The flow is to be described in the Cartesian coordinate system (x, y, z), with its origin at the location where the crossflow is introduced, where x, y and z denote the streamwise, normal and spanwise directions respectively, and they are all non-dimensionalized by $\delta = LR^{-1/2}$, the boundary-layer thickness at $x = 0$. The time variable t is normalized by δ/U_∞. The velocity (u, v, w) is non-dimensionalized by U_∞, while the non-dimensional pressure p is introduced by writing the dimensional pressure as $(p_\infty + \rho U_\infty^2 p)$, where p_∞ is a constant and ρ is the fluid density.

The profile of the Blasius boundary layer, $U_B(y, xR^{-1/2})$, is a function of y and $xR^{-1/2}$. Since both the imposed distortion and the instability wave evolve over much shorter streamwise length scales than that of the base flow, it suffices to approximate $U_B(y, xR^{-1/2})$ by its local profile at $x = 0$ via a Taylor expansion

$$U_B\left(y, xR^{-1/2}\right) = U_B(y, 0) + O\left(xR^{-1/2}\right). \tag{2.2}$$

In the following, $U_B(y, 0)$ will be written as $U_B(y)$. As $y \to 0$,

$$U_B(y) \to \lambda_0 y - \frac{\lambda_0^2}{48} y^4 + \ldots,$$

with $\lambda_0 \approx 0.33206$.

Let Λ denote the dimensional characteristic length scale over which the spanwise variation of the imposed distortion occurs (see figure 1). We assume that Λ is much larger than the local boundary-layer thickness δ, i.e.

$$\sigma \equiv \frac{\delta}{\Lambda} \ll 1,$$

so that the variation of the distortion can be described by the slow variable

$$Z = \sigma z. \tag{2.3}$$

A crossflow $\epsilon_M W_0(y, Z)$ is imposed at $x = 0$ by some excitation device. In the laboratory this may be achieved by inserting a thin wire with a non-uniform cross-section into the main part of the boundary layer. A small screen set normal to the wall, as in the experiments of Asai *et al.* (2000), probably produces a similar effect. The distortion produced by a small three-dimensional obstacle in a parallel

shear flow was investigated by Lighthill (1957). The body size was taken to be much smaller than the thickness of the background shear flow so that the viscous effect is confined in the vicinity of the obstacle, while in the majority of the flow field, the perturbation is governed by essentially inviscid dynamics. The effect of the obstacle was then represented as a point (mass) source. Lighthill obtained the solution for the case where the shear flow velocity nowhere vanishes. His solution therefore does not directly apply to boundary-layer flows, for which $U_B = 0$ at the wall, but Lighthill pointed out that such flows could be treated by retaining the viscous terms in the equations in a viscous sublayer near the wall. Another fact that needs to be carefully considered is that for a wire whose spanwise non-uniformity occurs over a longer length scale than the boundary layer thickness, its effect may be not treated as a point source. In any case, further work is needed to link $W_0(y, z)$ directly to the shape of the obstacle.

The mean-flow distortion due to a suddenly imposed crossflow $\epsilon_M W_0(y, Z)$ is analysed in detail by Goldstein & Wundrow (1995). They show that the solution for the distortion in the wall region (viscous sublayer) could be obtained without detailed knowledge of $W_0(y, Z)$ as a function of y. The mean-flow distortion evolves through several distinct stages along the streamwise direction. In the region $x = O(\sigma^{-1})$, the flow is fully interactive, but the distortion in this region is too weak to affect the instability. The important location for instability corresponds to $x = O(\sigma^3 R^{1/2})$, where the streamwise velocity profile of the distorted flow develops an inflection point in a viscous sublayer layer $y = O(\sigma)$, if the imposed crossflow has a magnitude $\epsilon_M \sim R^{-1/2}(\ln \sigma)^{-1}$. For a periodic distortion, a pair of oblique modes is in resonance with the distortion if the spanwise wavelength of the former is twice that of the latter. The characteristic streamwise wavelength of the instability modes is found to be comparable with that of the mean-flow distortion. The growth rate induced by the resonance has the same order of magnitude as that due to the viscosity if $\sigma = O(R^{-1/20})$, but is larger if $\sigma \gg R^{-1/20}$. In the latter case, the instability is primarily inviscid. The instability modes identified by them will be referred to as Goldstein–Wundrow (G–W) modes.

Further downstream, the streamwise velocity of the distortion continues to grow in proportion to x, but the wall region thickens like $x^{1/3}$, with the consequence that at a fixed value of y/σ, the curvature alteration eventually vanishes. As a result, inviscid modes with $O(\Lambda)$ streamwise length scale are stabilized due to the viscous diffusion of the wall region. Of course, this resonance-induced instability relies on the periodicity of the distortion in the first place, and does not take place if the distortion is non-periodic (e.g. localized).

The main interest of the present paper will be *localized distortions* since distortions of this form have been produced and studied in a number of experiments, as mentioned in § 1. It will be shown that an inviscid instability may occur in a region farther downstream than that considered by Goldstein & Wundrow (1995). This instability also arises in the case of a periodic distortion.

The region in which this instability operates, as well as its characteristic time and length scales, can be determined by a scaling argument based on three considerations. First, suppose that at a typical streamwise location $x \sim l \gg O(\sigma^3 R^{1/2})$, the wall layer has width $y \sim \hat{\sigma}$. Then the balance between the advection term $U_B \partial u/\partial x$ and the diffusion term $R^{-1/2}\partial^2 u/\partial y^2$ in the streamwise momentum equation implies that

$$\frac{\hat{\sigma}}{l} \sim \frac{R^{-1/2}}{\hat{\sigma}^2}. \tag{2.4}$$

Second, for the distortion to be able to induce an essentially inviscid instability, its curvature must be comparable to the $O(\hat{\sigma}^2)$ curvature of the Blasius flow in the wall layer, that is

$$\frac{\epsilon_D}{\hat{\sigma}^2} \sim \hat{\sigma}^2, \tag{2.5}$$

where ϵ_D stands for the magnitude of the streamwise velocity of the distortion. Note that for the steady streak considered herein, its curvature in the wall layer is $O(\epsilon_D/\hat{\sigma}^2)$, which is a factor $\hat{\sigma}^{-2}$ larger than that in the main region. This feature turns out to be important for the instability of the perturbed flow.

Third, given the likely appearance of an inflection point in the wall region of $y \sim \hat{\sigma}$, the classical Rayleigh scalings suggest that instability modes have $O(\hat{\sigma})$ streamwise wavenumbers, while their growth rates would be $O(\hat{\sigma}^4)$ (cf. Goldstein & Durbin 1986). The crucial balance which enables us to describe this instability is between the streamwise growth and spanwise modulation of the modes. This requires that

$$\hat{\sigma}^5 \sim \sigma^2. \tag{2.6}$$

We shall come back to this point later.

It follows from (2.4) and (2.6) that the instability will operate in the region where (see figure 1)

$$x \sim l = O\left(R^{1/2}\sigma^{6/5}\right),$$

and so we introduce the variable

$$\hat{x} = x/\left(\sigma^{6/5}R^{1/2}\right) \tag{2.7}$$

to describe the spatial development of the distortion. That $\hat{x} = O(1)$ corresponds to $xR^{-1/2} \sim \hat{\sigma}^3 \ll 1$ justifies the Taylor expansion (2.2). For $\hat{x} = O(1)$, the instability modes that the perturbed mean flow can support have streamwise wavelengths of $O(\sigma^{-2/5})$, much shorter than the $O(\sigma^{-1})$ spanwise length scale of the distortion. The phase speed is $O(\hat{\sigma})$ or $O(\sigma^{2/5})$, so that the frequency is $O(\sigma^{4/5})$. The distorted flow evolves over the length scale $x \sim \sigma^{6/5}R^{1/2}$, while the instability wave amplifies over the length scale $\hat{\sigma}^{-4}$. Therefore the dependence on $\hat{x}$ is parametric and the quasi-parallel flow approximation is valid provided that $\sigma^{6/5}R^{1/2} \gg \sigma^{-4}$, i.e. $\hat{\sigma} \gg R^{-1/14}$. This condition is certainly satisfied since we will assume that $\hat{\sigma} \geqslant R^{-1/20}$ so that the growth rate induced by the distortion is at least comparable with that by viscosity (see § 4). Without losing generality, in the rest of the paper we put

$$\hat{\sigma} = \sigma^{2/5}$$

on the basis of (2.6).

3. Solution for the mean-flow distortion

As mentioned earlier, the solution for the distortion was considered in detail by Goldstein & Wundrow (1995). In the immediate vicinity of forcing, the flow is complex and dependent on the initial forcing. However, an inflection point starts to emerge only sufficiently downstream, i.e. during the flow relaxation phase. The inflection point lies in a thin layer close to the wall. The velocity profile in this layer, which controls instability, becomes independent of the normal distribution of the initial forcing. For the purpose of the present paper, the required solution corresponds to the downstream limit of that given by Goldstein & Wundrow (1995), and acquires a similarity form, which describes both the normal distribution and the streamwise variation of the distortion.

In the main part of the boundary layer, the solution expands as

$$U = (U_B + O(\hat{\sigma}^3)) + \hat{\sigma}^4 U_D + \ldots, \tag{3.1}$$

$$V = R^{-1/2}[V_B + \hat{\sigma} V_D + \ldots], \tag{3.2}$$

$$W = \bar{\sigma} R^{-1/2} \sigma^{-3/5}[W_D + \ldots], \tag{3.3}$$

$$P = R^{-1} \sigma^{-9/5}[P_D + \ldots], \tag{3.4}$$

where for convenience we have put $\bar{\sigma} = (\ln \hat{\sigma})^{-1}$. The solution is exactly the same as that given by Goldstein & Wundrow (1995), namely

$$U_D = U_B'(D + \bar{\sigma}\hat{x} H_Z), \quad V_D = -U_B(D_{\hat{x}} + \bar{\sigma} H_Z), \quad W_D = W_0(y, Z), \tag{3.5}$$

where D is a function of $\hat{x}$ yet to be determined, and

$$H(y, Z) = \int_0^y \left[\frac{W_0(s, Z)}{U_B'(s)} - \frac{W_0(0, Z)}{\lambda_0 s} \right] \mathrm{d}s + \frac{W_0(0, Z)}{\lambda_0} \ln y. \tag{3.6}$$

As in Goldstein & Wundrow (1995), we assume that a generic condition

$$B(Z) \equiv W_0(0, Z) \neq 0$$

is satisfied by the distortion.

The streamwise and spanwise velocities are reduced to zero across a viscous wall region with a width of $O(\sigma^{2/5})$. The appropriate transverse variable is

$$Y = \frac{y}{\sigma^{2/5}}. \tag{3.7}$$

The mean flow expands as

$$U = \hat{\sigma} \lambda_0 Y + \hat{\sigma}^4 \left(\tilde{U} - \tfrac{1}{48} \lambda_0^2 Y^4 - \tfrac{1}{2} \lambda_0 \hat{x} Y \right) + \ldots, \tag{3.8}$$

$$V = \hat{\sigma}^2 R^{-1/2} \left(\tilde{V} + \tfrac{1}{4} \lambda_0 Y^2 \right) + \ldots, \tag{3.9}$$

$$W = R^{-1/2} \sigma^{-3/5} (\tilde{W} + \ldots). \tag{3.10}$$

The governing equations are found to be

$$\tilde{U}_{\hat{x}} + \tilde{V}_Y + \tilde{W}_Z = 0, \quad \lambda_0 Y \tilde{U}_{\hat{x}} + \lambda_0 \tilde{V} = \tilde{U}_{YY}, \quad \lambda_0 Y \tilde{W}_{\hat{x}} = \tilde{W}_{YY}. \tag{3.11}$$

Note that the pressure is absent from the equations. The solution to these equations satisfy the boundary conditions

$$\tilde{U} = \tilde{V} = \tilde{W} = 0 \quad \text{at} \quad Y = 0, \tag{3.12}$$

as well as the matching condition with the main-deck solution:

$$\tilde{U} \to \lambda_0 D + \bar{\sigma} \hat{x} B' \ln(\hat{\sigma} Y), \quad \tilde{W} \to \bar{\sigma} B \quad \text{as} \quad Y \to \infty. \tag{3.13}$$

Compared with the upstream solution of Goldstein & Wundrow (1995), the flow acquires a simpler structure as it relaxes downstream. The solution for $\tilde{U}$ and $\tilde{W}$ now simply corresponds to the first terms of (3.43) in Goldstein & Wundrow (1995), namely

$$\tilde{U} = \bar{\sigma} \hat{x} B'(Z) F(\eta), \quad \tilde{W} = \bar{\sigma} B(Z) G(\eta), \tag{3.14}$$

where the similarity variable is defined as

$$\eta = (\lambda_0 / \hat{x})^{1/3} Y. \tag{3.15}$$

The functions F and G satisfy the equations

$$F''' + \tfrac{1}{3} \eta^2 F'' - \tfrac{2}{3} \eta F' = -G, \quad G'' + \tfrac{1}{3} \eta^2 G' = 0. \tag{3.16}$$

They are subject to the boundary and matching conditions

$$F = F'' = G = 0 \quad \text{at} \quad \eta = 0, \tag{3.17}$$

$$F \to \ln\eta, \quad G \to 1 \quad \text{as} \quad \eta \to \infty. \tag{3.18}$$

By matching, the displacement function D in (3.5) is found as

$$D = \frac{\bar{\sigma}\hat{x}B'}{\lambda_0}\left\{\ln\left[\hat{\sigma}\left(\frac{\hat{x}}{\lambda_0}\right)^{1/3}\right] - C_1\right\}, \quad \text{with} \quad C_1 = \lim_{\eta\to\infty}(F - \ln\eta).$$

The displacement effect is transmitted, via the main layer, to the upper layer with $O(\sigma^{-1})$ thickness, where a pressure field of $O(R^{-1}\sigma^{-9/5})$ is induced. But this pressure is too weak to have a leading-order back effect on the viscous motion in the wall layer.

Goldstein & Wundrow (1995) found that the solution can be expressed in terms of special functions. Here we shall obtain it by solving the boundary-value problem (3.16)–(3.18) numerically.

4. Linear instability

When $\hat{x} = O(1)$, the distortion to the mean flow is still small in the whole flow field. An important point to note is that in the viscous wall region the curvature of the mean-flow distortion is comparable with that of the original Blasius flow, that is, the curvature of the total mean flow is altered by $O(1)$ in relative terms, and moreover becomes spanwise-dependent. This leads to a fundamental change of the instability property, which we now analyse.

As was indicated by the scaling argument in § 1, the admissible modes have streamwise wavenumbers of $O(\hat{\sigma})$, frequencies of $O(\hat{\sigma}^2)$ and growth rates of $O(\hat{\sigma}^4)$; so we introduce

$$\zeta = \hat{\sigma}\alpha x - \hat{\sigma}^2\omega t, \quad X = \hat{\sigma}^4 x, \tag{4.1}$$

to describe the rapid oscillation and the relatively slow amplification of the modes respectively, where α and ω are the scaled wavenumber and frequency. We expand α and the phase speed $c \equiv \omega/\alpha$ as

$$\alpha = \alpha_0 + \hat{\sigma}\alpha_1 + \ldots, \quad c = \frac{\omega}{\alpha} = c_0 + \hat{\sigma}c_1 + \ldots.$$

The most unstable modes that the perturbed flow can support must have a spanwise length scale comparable with that of the distortion. Modes with a shorter spanwise length scale may be treated in a quasi-planar manner, but they have smaller growth rates, and moreover their phase speeds would be a function of Z, contradicting the experimental observation of Asai *et al.* (2002) and Bakchinov *et al.* (1995) that the phase speed is constant along the spanwise direction. Such modes will be discarded. Therefore the spanwise variation of relevant instability waves is described by the variable Z. In the main part of the boundary layer, the modes take the form, to leading order,

$$u = \epsilon A(X, Z)\bar{u}_1(y)\,\mathrm{e}^{\mathrm{i}\zeta} + \text{c.c.} + \ldots, \tag{4.2}$$

$$v = -\epsilon\hat{\sigma}\alpha\mathrm{i}A(X, Z)\bar{v}_1(y)\,\mathrm{e}^{\mathrm{i}\zeta} + \text{c.c.} + \ldots, \tag{4.3}$$

$$w = \epsilon\hat{\sigma}^{5/2}A_Z(X, Z)\bar{w}_1(y)\,\mathrm{e}^{\mathrm{i}\zeta} + \text{c.c.} + \ldots, \tag{4.4}$$

$$p = \epsilon\hat{\sigma}A(X, Z)\bar{p}_1(y)\,\mathrm{e}^{\mathrm{i}\zeta} + \text{c.c.} + \ldots, \tag{4.5}$$

where ϵ represents the magnitude of the modes, and A is the amplitude function.

Since the wavelengths of the instability modes are long compared with the boundary-layer thickness, the linear instability problem is governed by a five-zoned asymptotic structure that is akin to that for the upper-branch instability of the unperturbed Blasius boundary layer (cf. Bodonyi & Smith 1981; Goldstein & Durbin 1986). It consists of the upper layer, the main layer, the Tollmien layer, the viscous Stokes layer as well as the critical layer centred at the position where the basic flow velocity equals the phase velocity c. These regions have thickness of order $\hat{\sigma}^{-1}$, 1, $\hat{\sigma}$, $R^{-1/4}\hat{\sigma}^{-1}$ and $\hat{\sigma}^4$ respectively. Here the width of the critical layer is determined by requiring the small growth rate to remove the critical-layer singularity, i.e. the non-equilibrium effect appears in the leading-order critical-layer equations.

The solution in each of these regions can be obtained by following what is now a fairly routine procedure (see e.g. Wu, Stewart & Cowley 1996). Matching these solutions gives the leading-order dispersion relation

$$c_0 = \frac{\alpha_0}{\lambda_0}, \tag{4.6}$$

and the relation to determine the growth rate

$$A_X - \frac{\mathrm{i}}{4\alpha_0} A_{ZZ} = (c^+ - c^-) + \left[\frac{\lambda_0^2}{2R^{1/4}\hat{\sigma}^5 (2\alpha_0 c_0)^{1/2}} + \mathrm{i}\chi_0 \right] A, \tag{4.7}$$

where $(c^+ - c^-)$ is the jump across the critical layer, and χ_0 is a real constant which does not have any effect on instability. In the linear regime ($\epsilon \ll 1$),

$$c^+ - c^- = \pi c_0 Y_c \Omega A, \tag{4.8}$$

where $Y_c = c_0/\lambda_0$ is the scaled critical level, and Ω is the curvature of the perturbed flow at the critical level

$$\Omega = -\frac{c_0^2}{4} + \Omega_c(Z), \quad \text{with} \quad \Omega_c = \tilde{U}_{YY}(Y_c, Z). \tag{4.9}$$

Inserting (4.8) into (4.7) gives

$$A_X - \frac{\mathrm{i}}{4\alpha_0} A_{ZZ} = (\gamma_0 + \gamma(Z;\hat{x}))A, \tag{4.10}$$

where

$$\gamma_0 = -\frac{\pi c_0^4}{4\lambda_0} + \frac{\lambda_0^2}{2R^{1/4}\hat{\sigma}^5 (2\alpha_0 c_0)^{1/2}}, \tag{4.11}$$

$$\gamma(Z;\hat{x}) = \frac{\pi c_0^2}{\lambda_0} \Omega_c(Z) = \pi c_0^2 \left(\frac{\hat{x}}{\lambda_0} \right)^{1/3} F''(\eta_c) B'(Z) \equiv \tilde{\gamma}(\hat{x}) B'(Z), \tag{4.12}$$

with $\eta_c = (c_0/\lambda_0)(\lambda_0/\hat{x})^{1/3}$. Here use has been made of (3.14) and (3.15), and the logarithmic factor $\bar{\sigma}$ has been absorbed into the definition of B. Obviously γ_0 is the growth rate in the absence of the distortion, with the second term in γ_0 representing the contribution from the viscous Stokes layer, which is the sole instability mechanism when the distortion is absent.

The derivation of (4.10) is underpinned by the property that the major curvature alteration occurs in a wall layer. As is indicated by (4.10), in this case the curvature alteration in the wall region is the sole quantity that characterizes the instability of the perturbed flow; the distortion in the main part of the boundary layer turns out to be largely irrelevant. As we will see in Part 2, the Klebanoff modes do not share

the property of the distortion considered here, and consequently a separate analysis is required.

Equation (4.10) can be viewed as a Schrödinger equation with a purely imaginary potential $i\gamma(Z)$. It admits solutions of the form

$$A = \Phi(Z)\, e^{(a+\gamma_0)X}, \tag{4.13}$$

where a is a complex constant, and $\Phi(Z)$ satisfies

$$\Phi_{ZZ} = 4i\alpha_0(\gamma(Z) - a)\Phi. \tag{4.14}$$

The above equation together with appropriate boundary conditions forms an eigenvalue problem to determine a. Clearly, the real part of a represents the *excess growth rate* induced by the distortion or streak. As will be shown below, the Schrödinger operator with a purely imaginary potential has a complex spectrum a.

Depending on the size of $\hat{\sigma}$, the instability may be of a quite different nature. Equations (4.11) and (4.12) indicate that the growth rate due to the viscosity is negligible if $\hat{\sigma} \gg R^{-1/20}$ or equivalently if the magnitude of the streamwise velocity of the distortion satisfies

$$\epsilon_D \gg R^{-1/5}.$$

This implies that when the distortion exceeds a threshold order of magnitude, the instability becomes essentially inviscid with the growth rate

$$\kappa \equiv a_r - \frac{\pi c_0^4}{4\lambda_0}, \tag{4.15}$$

although it may be argued that inclusion of the viscous growth in this case would give a more general result.

When $\epsilon_D \sim R^{-1/5}$, the distortion provides a modification to the viscous growth rate, and the modes may therefore be viewed as a kind of modified T–S wave, even though in the case of localized distortion they are not directly linked to the usual T–S waves that exist in the zero-distortion limit; see further discussion below.

Thus far the localized and periodic distortions have been treated in a unified manner. Subsequent analyses, however, have to distinguish these two cases.

4.1. *Localized distortion*

For a localized $\gamma(Z)$, the boundary conditions are

$$\Phi(Z) \to 0 \quad \text{as} \quad Z \to \pm\infty,$$

or more precisely

$$\Phi(Z) \to \exp\big(\mp(-4i\alpha_0 a)^{1/2} Z\big) \quad \text{as} \quad Z \to \pm\infty, \tag{4.16}$$

where the square root is taken to be the one with a positive real part.

A general result similar to the familiar 'semi-circle theorem' can be derived as follows. Multiplying (4.14) by Φ and integrating from $-\infty$ to ∞, and performing integration by parts on the left-hand side, we obtain

$$-\int_{-\infty}^{\infty} |\Phi_Z^*|^2 \, \mathrm{d}\, Z = 4i\alpha_0 \int_{-\infty}^{\infty} (\gamma - a)|\Phi|^2 \, \mathrm{d}\, Z, \tag{4.17}$$

which implies that

$$\int_{-\infty}^{\infty} [\gamma - \mathrm{Re}(a)]|\Phi|^2 \, \mathrm{d}\, Z = 0.$$

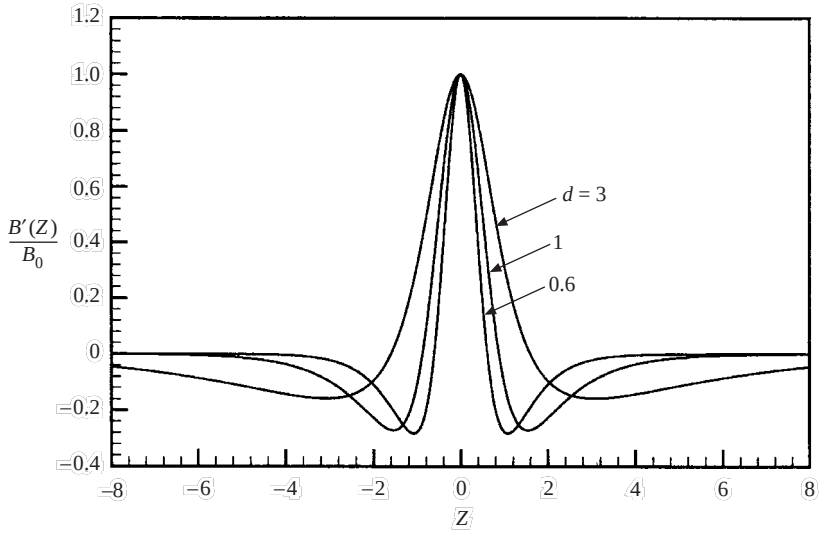

FIGURE 2. Shape of the distortion (4.19) for $d = 0.6, 1, 3$.

It can therefore be deduced that

$$\min \gamma(Z) < \mathrm{Re}(a) < \max \gamma(Z). \tag{4.18}$$

In fact the same result holds for the periodic case (see below).

The eigenvalue problem (4.14) with (4.16) is solved numerically for a spanwise distribution of the form

$$B'(Z) = B_0 \,\mathrm{sech}(Z/d) \tanh Z, \tag{4.19}$$

where d is a measure of the spanwise length scale of the distortion. Figure 2 displays the shape for three values of d. The distribution is quite similar to that in the experiments of Asai *et al.* (2000, 2001). A salient feature is that the distortion changes its sign in the spanwise direction, indicating that in conjunction with a dominant low-speed streak, there is also a region where the flow is accelerated by the distortion. This is the consequence of the fact that the spanwise velocity of the distortion must vanish at $\pm\infty$, which imposes the constraint

$$\int_{-\infty}^{\infty} \gamma(Z)\,\mathrm{d}Z = 0.$$

The effect of the streamwise variation of the distortion on the instability is characterized by $\tilde{\gamma}(\hat{x})$, but in order to have a grasp of the general properties of the problem, calculations were first performed for the artificial case where $\tilde{\gamma} = 1$. The variation of a_r with B_0 is plotted in figure 3 for two fixed values of d. It shows that $a_r > 0$ when the distortion exceeds a threshold magnitude B_c. Below B_c, the localized mode does not exist. Instead there exists a continuous spectrum for which a is purely imaginary so that Φ is only bounded at $Z = \pm\infty$. The continuous spectrum can be viewed as the usual T–S waves whose shape is deformed by $\gamma(z)$, but whose growth rates are not affected. Though no detailed study has been made of the continuous spectrum, it is clear that it eventually turns into the usual T–S waves when $B_0 \to 0$. The existence of a threshold means that the localized modes do not directly reduce to the usual T–S waves as the distortion is reduced; instead they merge into the continuous spectrum at B_c.

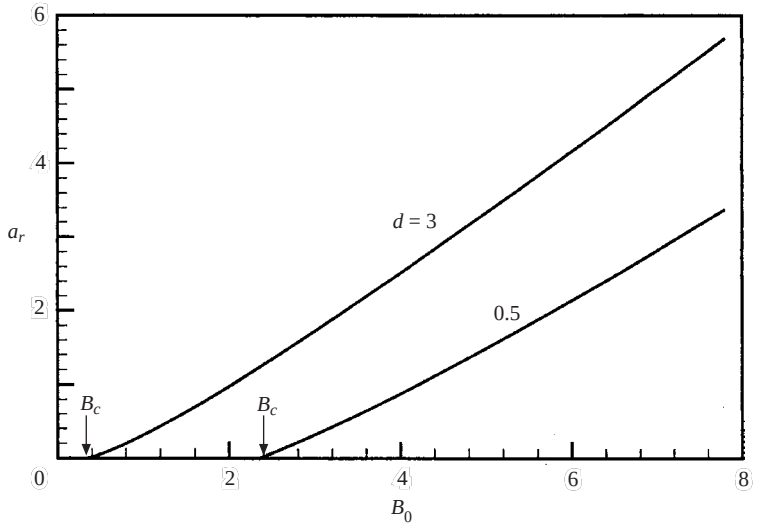

FIGURE 3. Variation of the excess growth rate a_r with the distortion strength B_0. B_c indicates the threshold magnitude for the localized mode to exist.

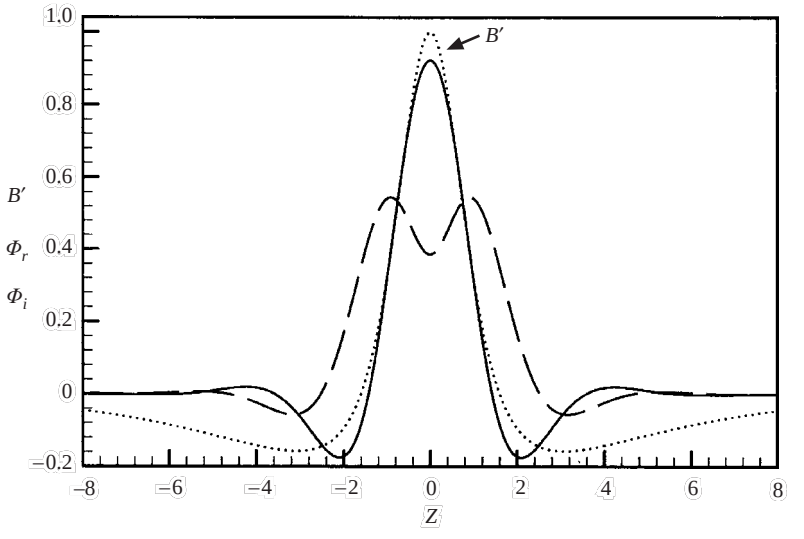

FIGURE 4. A typical spanwise distribution of the eigenfunction normalized by its maximum ($d = 3$ and $B_0 = 4$). Solid line: real part Φ_r; dashed line: imaginary part Φ_i; dotted line: the mean-flow distortion.

A typical distribution of the eigenfunction Φ is shown in figure 4. Clearly, the instability mode is confined to the region of the mean-flow distortion, and decays rapidly away from it. The mode is symmetric or varicose in nature. No anti-symmetric (or sinuous) mode has been found. Asai *et al.* (2002) attributed the varicose modes to the inflection point in the normal direction $U_{YY} = 0$, and the sinuous modes to the spanwise inflection point $U_{ZZ} = 0$. The former term is included in our theory, but the latter is ignored. That the varicose modes are absent in our model is consistent with Asai *et al.*'s conclusion, and also may be taken as indicating the importance of U_{ZZ} in inducing the sinuous modes.

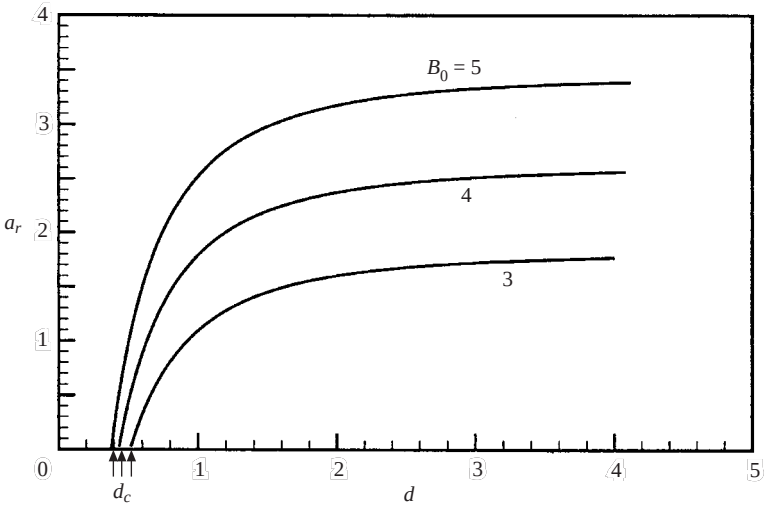

FIGURE 5. Variation of the excess growth rate a_r with d, the spanwise length scale of the distortion. Here d_c indicates the threshold scale for a localized mode to exist.

Figure 5 shows the variation of a_r with d. For each fixed B_0, there exists a threshold d_c above which a localized mode comes into existence. The growth rate increases with the spanwise length scale d, and quickly saturates at the 'two-dimensional limit' when d is large enough. This conclusion is in agreement with the experimental findings of Asai *et al.* (2002), although in their experiments the distortion has a rather large magnitude. It seems reasonable to suggest that the present simple theory captures some generic features of the secondary instability caused by a steady streak.

Next we present the instability results for the particular distortion considered in § 3, for which $\tilde{\gamma}$ depends on $\hat{x}$, and is evaluated by solving (3.16)–(3.18) numerically. It is found that $F > 0$ but $F'' < 0$, and as a result $\tilde{\gamma} < 0$ (see (4.12)). Therefore according to the result shown in figure 3, inviscid instability is possible only for $B_0 < 0$, i.e. when the distortion is characteristic of a low-speed streak. The present simple model is consistent with this fundamental observation.

For a given B_0, the inviscid growth rate $\kappa(\omega, \hat{x})$ as defined by (4.15) will be a function of $\hat{x}$ and $\omega = \alpha_0 c_0$, the frequency of the instability mode. As is shown in figure 6(*a*), in the streamwise region in which the distortion is significant, the perturbed flow supports a band of instability modes, which lead to oscillation of the streak. In figure 6(*b*), we plot the variation of the growth rate κ with $\hat{x}$ for three typical values of ω. As is illustrated, a mode with a suitable frequency experiences amplification in a finite streamwise region, beyond which it decays. The spatial extent and the frequency range of the unstable modes can be best demonstrated by plotting the contours of the growth rate $\kappa(\omega, \hat{x})$ in the $(\hat{x}, \omega)$-plane (figure 7). For $B_0 = -6$, the perturbed flow is unstable in the streamwise window between $\hat{x} \approx 1.2$ and $\hat{x} \approx 7.4$ (figure 7*a*). The unstable frequency band varies with $\hat{x}$, but roughly speaking the overall range is between $\omega = 0.3$ and 0.7. The frequency of the most unstable modes at the upstream end is fairly small, but increases with downstream distance, implying progressively more rapid streak oscillations. Figure 7(*b*) displays the growth-rate contours for $B_0 = -7$, and it indicates that for stronger distortion, the unstable region becomes more spatially extended and the unstable modes become more broad-band.

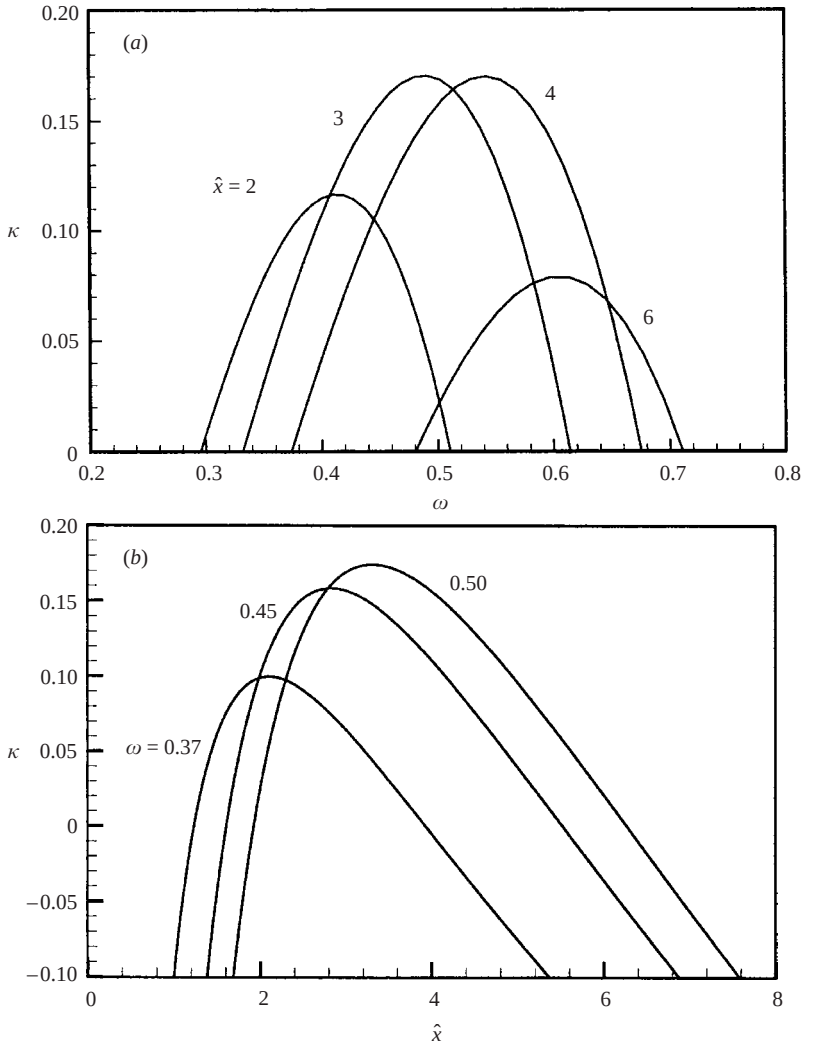

FIGURE 6. Inviscid growth rates of localized modes for $B_0 = -6$. (*a*) Growth rate κ as a function of the frequency ω at typical streamwise locations. (*b*) Variation of κ with $\hat{x}$ for a fixed frequency ω.

4.2. *Periodic distortion*

Consider now a periodic distortion, i.e. $\gamma(Z) = \gamma(Z + l_d)$, where l_d is the period. Floquet theory suggests that Φ takes the form $\Phi = \bar{\Phi}(Z)e^{i\mu Z}$, where $\bar{\Phi}(Z)$ is a periodic function satisfying

$$\bar{\Phi}_{ZZ} + 2i\mu\bar{\Phi}_Z - \mu^2\bar{\Phi} = 4i\alpha_0(\gamma(Z) - a)\bar{\Phi}, \tag{4.20}$$

and μ is a real constant (in order for Φ to be bounded as $Z \to \pm\infty$). Result (4.18) then can immediately be derived by a procedure similar to that for a localized distortion with the only difference being that the integration is now over a single period of the distortion.

In general, $\gamma(Z)$ has the Fourier representation $\gamma(Z) = \sum_{n=1} \gamma_n \cos(2n\beta Z)$, where $2\beta = 2\pi/l_d$ is the wavenumber of the distortion, but for simplicity, we

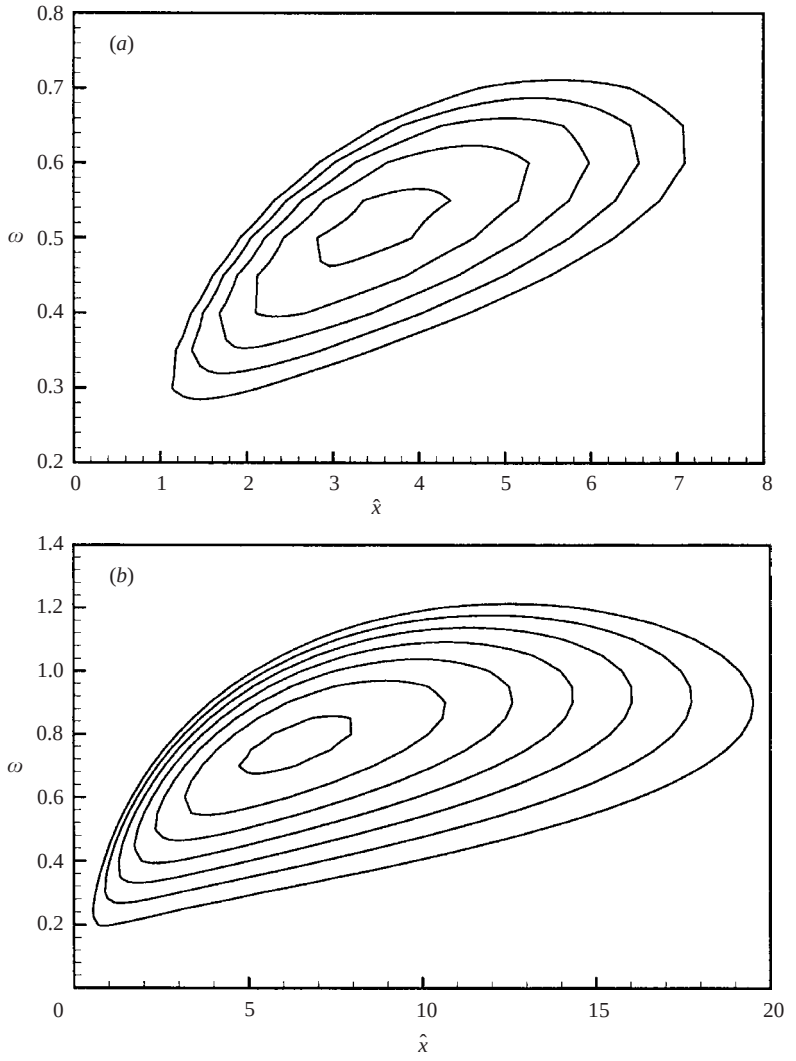

FIGURE 7. Contours of growth rates for (*a*) $B_0 = -6$ and (*b*) $B_0 = -7$. The outermost contour corresponds to the neutral curve $\kappa(\omega, \hat{x}) = 0$. The enclosed region represents the spatial and spectral extent of the instability.

consider

$$\gamma = \gamma_1 \cos(2\beta Z). \tag{4.21}$$

We can expand $\bar{\Phi}$ as a Fourier series so that

$$\Phi(Z) = \sum_{n=-\infty}^{\infty} f_n e^{i(n\beta+\mu)Z}. \tag{4.22}$$

Equation (4.20) describes a parametric resonance, which may be of subharmonic or fundamental form. The former corresponds to $n = 1, 3, 5, \ldots$ and the latter to $n = 0, 2, 4, \ldots$ in (4.22). These two cases can be treated on an equal footing by allowing $0 \leqslant \mu \leqslant 1$. Inserting (4.21)–(4.22) into (4.16) leads to a system of linear simultaneous equations of infinite dimension for f_n, which is truncated at a finite

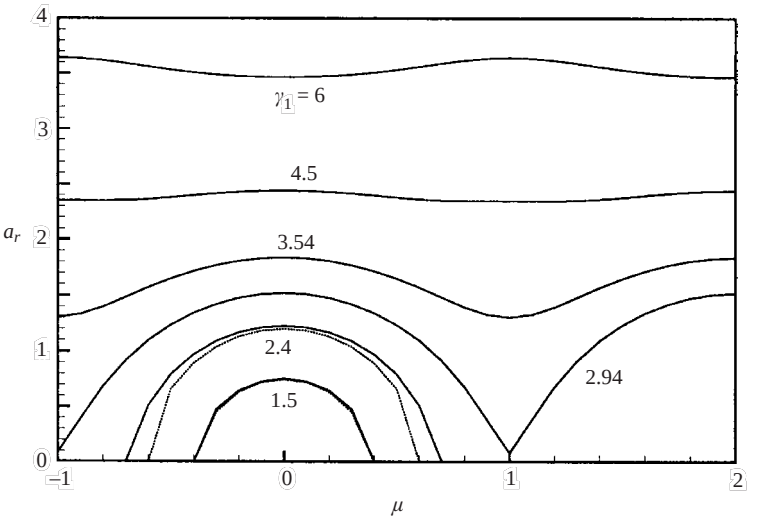

FIGURE 8. Excess growth rates of Floquet modes, a_r, as a function of μ for $\gamma_1 = 1.5, 2.4, 2.94, 3.5, 4.5, 6$. The subharmonic and fundamental parametric resonances correspond to the vicinities of $\mu = 0$, 1 respectively. The latter exists only when the distortion exceeds a threshold.

order. The resulting finite-dimensional system is solved numerically to determine a in terms of μ.

For a weak distortion ($\gamma_1 \ll O(1)$), a perturbation analysis can be performed to give some analytical insight. Subharmonic parametric resonance occurs if $a \sim -\mathrm{i}\beta^2$. The appropriate expansions are

$$\left.\begin{aligned} a &= -\mathrm{i}\beta^2 + \gamma_1 a_1 + \ldots, \\ \bar{\Phi} &= \bar{\Phi}_0(Z) + \gamma_1 \bar{\Phi}_1(Z) + \ldots, \\ \mu &= \gamma_1 \mu_1 + \ldots. \end{aligned}\right\} \tag{4.23}$$

Substitution of (4.23) into (4.20) gives rise to a sequence of equations for $\bar{\Phi}_0$, $\bar{\Phi}_1$, etc. At leading-order, $\bar{\Phi}_0$ is found to be a linear combination of $\mathrm{e}^{\pm \mathrm{i}\beta Z}$, while the requirement that $\bar{\Phi}_1$ is free of any 'secular term' leads to

$$a_1 = \tfrac{1}{4} - 4\mu_1^2\beta^2. \tag{4.24}$$

This relation indicates that the most unstable mode has the growth rate

$$a_r = \tfrac{1}{2}\gamma_1.$$

The perturbation analysis indicates that the subharmonic modes exist for a arbitrarily small distortion, and these modes reduce to the usual T–S waves as the distortion strength goes to zero.

A similar perturbation analysis can be carried out for the fundamental resonance. However, we find that to $O(\gamma_1^2)$, a is purely imaginary, and it appears that unlike subharmonic resonance, parametric resonance of fundamental type does not occur for an arbitrarily small $\gamma(Z)$ for the system under investigation. This will be confirmed by our numerical solutions to (4.20).

The excess growth a_r as a function of μ is presented in figure 8 for several values of γ_1. The subharmonic and fundamental resonances correspond to the vicinity of $\mu = 0$ and $\mu = 1$ respectively. For small and moderate γ_1, the subharmonic resonance

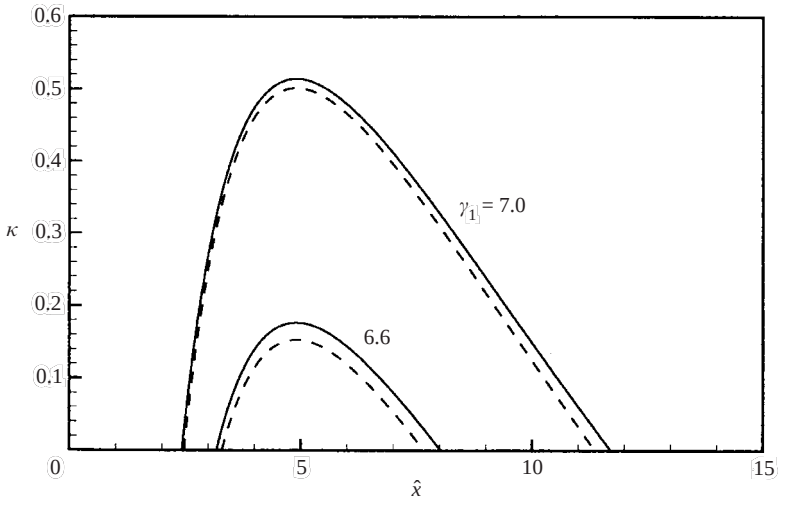

FIGURE 9. Growth rates of typical Floquet modes ($\omega = 0.65$) vs. $\hat{x}$ for the distortion considered in § 3. Parameters: $\gamma_1 = 6.6$, 7. Solid lines: fundamental modes; dashed lines: subharmonic modes.

dominates, with the maximum excess growth being given by $\mu = 0$. It turns out that the asymptotic approximation (4.24) is indistinguishable from the numerical solution for γ_1 up to 1.5, and is reasonably accurate for even larger γ_1 provided μ is not too large. The fundamental resonance occurs only when γ_1 exceeds a threshold magnitude γ_c. In this case, $\gamma_c \approx 2.92$. Close to the onset of the fundamental resonance, the growth is a minimum, and only when γ_1 is sufficiently large does the growth becomes a weak maximum. In this range of γ_1, a very broad band of instability modes all have comparable growth rates. These modes in general are quasi-periodic in Z.

We also calculated the growth rate κ for the distorted flow considered in § 3. Figure 9 shows the variation of κ with $\hat{x}$ for a fixed frequency. The values of γ_1 here were chosen so that the excess growth is large enough to overcome the decay rate associated with the curvature of the unperturbed Blasius profile. This requires a fairly large γ_1, for which the parametric resonance leads to broad-band instability. For weaker distortions, κ is negative, although they still induce an excess growth rate $a_r > 0$.

5. Nonlinear instability

As an instability mode amplifies, nonlinear effects may become important. For an instability wave with an asymptotically small growth rate, it is now well recognized that the dominant nonlinear interactions will first take place within the critical layer to produce a velocity jump across this layer. For reviews, see e.g. Goldstein (1994) and Cowley & Wu (1994).

For the present problem, the nonlinear jump becomes comparable with the linear jump when

$$\epsilon = \hat{\sigma}^{17/2}. \tag{5.1}$$

We shall assume that the Reynolds number R scales with $\hat{\sigma}$ as

$$R^{-1/2} = r\hat{\sigma}^{13} \tag{5.2}$$

so that the viscous diffusion appears as a leading-order effect in the critical layer, where r is a parameter of order one, reflecting the effect of viscosity. In passing, we note that the the experiments of Bakchinov *et al.* (1995), which investigate the instability of a Blasius boundary layer subject to a spanwise-dependent distortion, point to the existence of a well-defined critical layer, in which the mode attains its largest magnitude.

The nonlinear jump is the same as that calculated in Wu (1993) and Wu *et al.* (1996). Inserting that jump into (4.7), we obtain the amplitude equation that describes the nonlinear instability of the perturbed flow

$$A_X - \frac{\mathrm{i}}{4\alpha_0} A_{ZZ} = (\gamma_0 + \gamma(Z))A + \mathrm{i}N(X, Z), \tag{5.3}$$

where the nonlinear term

$$\begin{aligned} N = \int_0^\infty \int_0^\infty K(\xi, \eta|s)\{&\xi^3 A(X-\xi)A(X-\xi-\eta)A^*_{ZZ}(X-2\xi-\eta) \\ &+ \xi^2\eta A(X-\xi)[A(X-\xi-\eta)A^*_Z(X-2\xi-\eta)]_Z \\ &+ \xi^3[A(X-\xi)A(X-\xi-\eta)A^*_Z(X-2\xi-\eta)]_Z\}\,\mathrm{d}\xi\,\mathrm{d}\eta, \end{aligned} \tag{5.4}$$

with

$$K(\xi, \eta|s) = \exp(-s(2\xi^3 + 3\xi^2\eta)), \quad s = \tfrac{1}{3}\alpha_0^2\lambda_0^2 r.$$

In (5.3), the amplitude function has been suitably renormalized so that the coefficient multiplying iN is unity. The amplitude A should match to the linear solution upstream, and so we have

$$A \to \Phi(Z)\mathrm{e}^{(a+\gamma_0)X} \quad \text{as} \quad X \to -\infty. \tag{5.5}$$

It is worth pointing out that the 'initial condition' can be applied at $-\infty$, because a localized eigenmode exists in the linear limit. Equation (5.3) with $\gamma \equiv 0$ also describes the nonlinear development of modulated instability waves on some spanwise-uniform shear flows, but there the initial condition has to be imposed at $X = 0$ (Wu 1993).

The nonlinear amplitude equation (5.3) was first solved for the localized distortion. The mode was chosen to be the most unstable one in figure 7(b), which is at $\hat{x} \approx 6.5$ and has a frequency $\omega = 0.8$. The nonlinear evolution of $|A(X, 0)|$, the amplitude on the symmetry plane, is shown in figure 10(a) for three viscous parameter values. Nonlinearity enhances the amplification, and apparently leads to a singularity at a finite distance downstream. Viscosity delays the formation of the singularity but cannot eliminate it. Figure 10(b) shows that the nonlinear effect deforms the shape of the mode, and a singularity of self-focusing type appears to be forming at $Z = 0$. When focusing occurs, the linear term $\gamma(Z)A$ becomes secondary so that the main balance becomes the same as that for the equation in Wu (1993). It may therefore be expected that the singularity would have the same structure as described in Wu (1993), where evidence supporting the proposed singularity was given. However a full verification of the singularity proved hard, and has to be left for future work.

In the case of a periodic distortion, the nonlinear development of a fundamental mode is shown in figure 11(a). The overall features are similar to the isolated case (cf. figure 10a). The spanwise deformation of the mode is monitored by plotting the real and imaginary parts of A against Z (figure 11b). The mode in the initial linear stage is quite spread out, but nonlinearity causes it to focus towards the centre. This implies that although the linear Floquet instability mechanism is 'collective', in the nonlinear regime, the instability appears to be local in character. A comparison with

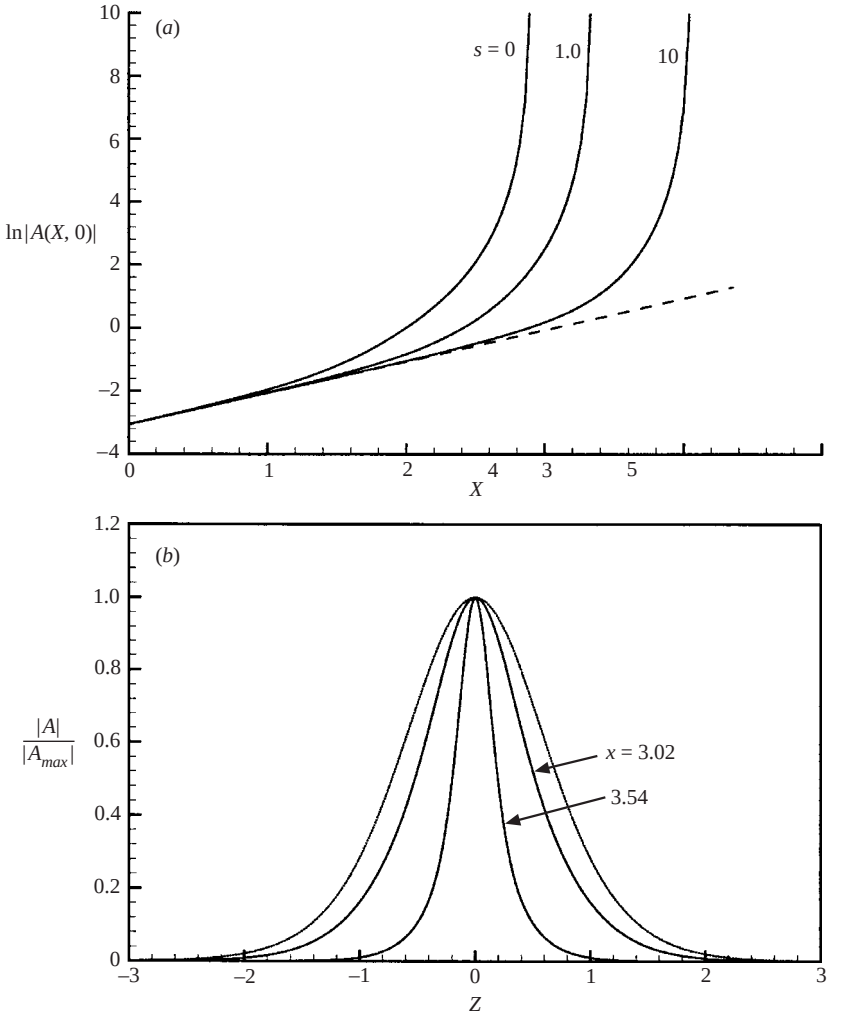

FIGURE 10. Nonlinear evolution of the most unstable localized mode in figure 7(*b*) ($\omega = 0.8$, $\hat{x} = 6.5$). (*a*) The amplitude on the symmetry plane $\ln|A(X,0)|$ vs. X for $s = 0$ (purely inviscid case), 1 and 10. The dashed line represents the linear limit. (*b*) Spanwise distribution of $|A|$ at $X = 3.02,\ 3.54$ for $s = 1$.

figure 4 indicates that the shape of the Floquet mode in the nonlinear regime very much resembles that of a linear local mode.

A periodic distortion supports the G–W mode as well as the Floquet mode described above. A discussion of their relation is now in order. At a fixed streamwise location, the instability properties are directly controlled by two parameters, σ and ϵ_D, which characterize respectively the spanwise wavelength and the local magnitude of the streamwise velocity of distortion. For a fixed spanwise wavelength (or equivalently σ), the G–W mode requires a smaller threshold, of $O(\sigma^4)$, and therefore should emerge first. As ϵ_D increases, the characteristic streamwise wavenumber and growth rate of the G–W mode increase as well. The mode therefore becomes progressively 'two-dimensional', and turns into the Floquet mode when $\epsilon_D \sim \sigma^{8/5}$. If ϵ_D is held fixed, then (2.5) and (2.6) imply that distortion with a relatively long spanwise length, of $O(\epsilon_D^{5/8})$,

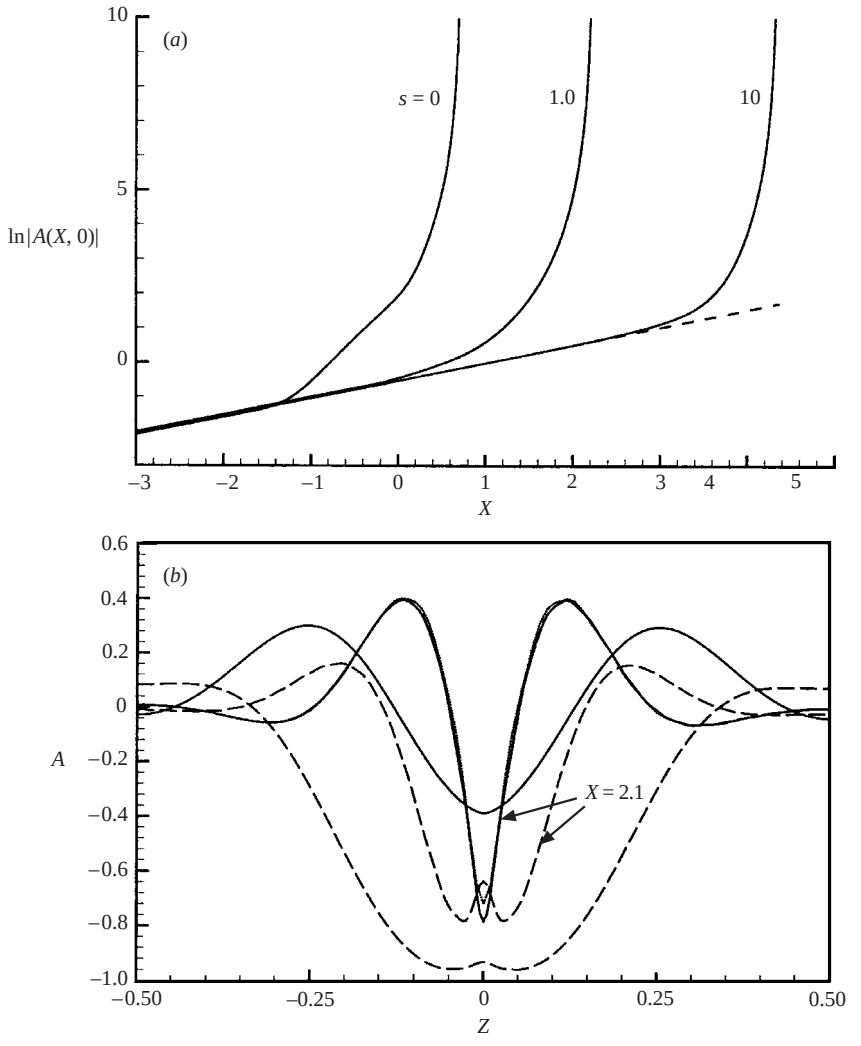

FIGURE 11. Nonlinear evolution of the most unstable (fundamental) mode in figure 9(*b*) ($B_0 = -7$, $\hat{x} = 6.0$, $\omega = 0.65$). (*a*) The amplitude on the symmetry plane $\ln|A(X,0)|$ vs. X for $s = 0$ (purely inviscid case), 1 and 10. (*b*) Spanwise distribution of $|A|$ (for $s = 1$) in the linear and nonlinear regimes ($X = 2.10$). Solid lines: real part of A; dashed lines: imaginary part of A. The calculations used 62 Fourier terms. The result obtained with 42 Fourier terms is shown by the dotted line that almost coincides with the solid line.

supports the Floquet mode, while distortion with a relatively short wavelength, of $O(\epsilon_D^{1/4})$ according to Goldstein & Wundrow (1995), supports the G–W mode.

The relation between the Floquet and the G–W modes can be better seen by considering where they emerge and how they evolve for the same distortion, whose overall magnitude is determined by the magnitude of the imposed crossflow. In particular if the magnitude is as specified in the present study (see (3.10)), the Floquet mode appears in the region where $x \sim \sigma^{6/5} R^{1/2}$, but the G–W instability operates at upstream locations where $x \sim \sigma^3 R^{1/2}$. In fact the upstream the G–W mode gradually evolves into a Floquet mode (if the former does not become nonlinear).

6. Discussion and conclusions

In this paper, we have shown that the instability of a Blasius boundary layer can be significantly modified and even fundamentally altered by certain three-dimensional distortions of relatively small amplitude. This occurs when the curvature of the distortion becomes comparable to that of the Blasius profile in a suitable vicinity of the wall. A self-consistent asymptotic theory is presented for distortions with spanwise length scale larger than the boundary-layer thickness. Both localized and periodic distortions are considered, and they can be treated on the same basis. The instability of the perturbed flow is shown to be governed by a remarkably simple system, a Schrödinger equation with a purely imaginary potential.

In the case of a moderate distortion which induces an excess growth rate comparable to that due to viscosity, the instability modes can be viewed as kinds of modified T–S waves. This modification is non-trivial however, because the spanwise shape is dictated by the distortion. For a localized distortion, the modes do not reduce to the usual T–S waves in the zero-distortion limit.

When the strength of the distortion exceeds a threshold order of magnitude, essentially inviscid instability arises. A local distortion may induce a localized instability mode, while a periodic distortion leads to quasi-periodic modes through a parametric resonance. The characteristic streamwise wavelength of the instability modes is much shorter than the spanwise length scale of the distortion, and their characteristic frequency is higher than those of typical T–S waves on Blasius flow. For the particular distortion considered in this paper, the instability occurs only when the flow features a low-speed streak. Also, the instability occurs in a limited streamwise window, and hence on a purely linear basis, the instability modes will die out. However, they can enter a nonlinear regime if a significant magnitude is attained. The continued nonlinear development of these modes is governed by a modified form of the evolution equation derived by Wu (1993), and the nonlinear effect is found to be strongly destabilizing, causing the amplitude to break down in the form of a finite-distance singularity. In the case of an isolated distortion, the instability should lead to patches of streak oscillation, which may well break down into turbulent spots.

While the theory is built upon a set of rather restricted asymptotic relations, it does appear to be capable of capturing qualitatively some major laboratory observations. For instance, the existence of a threshold magnitude and the occurrence of oscillation patches are in agreement with the conclusions of Hamilton & Abernathy (1994). As mentioned above, the theoretical prediction that the growth rate increases with the spanwise length scale of the distortion is consistent with the measurements of Asai *et al.* (2002). The predicted high-frequency nature of the inviscid unstable modes, as well as the excess growth exhibited by T–S waves, are in line with the findings of Bakchinov *et al.* (1995).

It should be noted that the distortions in the experiments are comparable with the basic Blasius flow so that they must be governed by nonlinear as opposed to the linear equations employed in our theory. Based on the above broad agreement, it seems reasonable to argue that the nonlinear structure of the distortion should not affect the qualitative features of the instability, and that the present simplified model keeps the key physics of the instability. From the qualitative point of view, the failure to describe the sinuous instability mode seems to be the only obvious shortcoming of the model.

The work of X.W. was carried out during his sabbatical in 2001 at Tianjin University (China), ICASE NASA Langley and the Center for Turbulence Research, Stanford

University (USA). The hospitality and financial support of these institutions are gratefully acknowledged. It is a great pleasure to thank Professors H. Zhou, Parviz Moin, W. C. Reynolds and Paul Durbin for helpful discussions. Thanks also go to Dr M. Asai for making available a preprint of his experimental results, and to Dr Meelan Choudhari and Professor Peter Bradshaw for their detailed comments on an earlier version of the work.

REFERENCES

Andersson, P., Brandt, L., Bottaro, A. & Henningson, D. S. 2001 On breakdown of boundary layer streaks. *J. Fluid Mech.* **428**, 29–60.

Asai, M., Fukuoka, A. & Nishioka, M. 2000 Experimental investigation of the instability of low-speed streak in a boundary layer. In *Mechanics for the New Millenium: Proc. 20th Intl Congr. on Theoretical and Applied Mechanics, Chicago* (ed. H. Aref & J. W. Phillips). Kluwer.

Asai, M., Minagawa, M. & Nishioka, M. 2002 The instability and breakdown of a near-wall low-speed streak. *J. Fluid Mech.* **455**, 289–314.

Bakchinov, A. A., Grek, G. R., Klingmann, B. G. B. & Kozlov, V. V. 1995 Transition experiments in a boundary layer with embedded streamwise vortices. *Phys. Fluids* **7**, 820–832.

Bennett, J. & Hall, P. 1988 On the secondary instability of Taylor–Görtler vortices to Tollmien–Schlichting waves in fully developed flows. *J. Fluid Mech.* **186**, 445–469.

Blair, M. F. 1992 Boundary-layer transition in acceleration flows with intense freestream turbulence Part I—disturbance upstream of transition onset. *Trans. Asme: J. Fluids Engng* **114**, 313–321.

Bodonyi, R. J. & Smith, F. T. 1981 The upper-branch stability of the Blasius boundary layer, including non-parallel flow effects. *Proc. R. Soc. Lond.* A **373**, 65–92.

Bradshaw, P. 1965 The effect of wind-tunnel screens on nominally two-dimensional boundary layers. *J. Fluid Mech.* **22**, 679–687.

Cowley, S. J. & Wu, X. 1994 Asymptotic methods and solutions in transition modelling. In *Progress in Transition Modelling*, *AGARD Rep.* 793.

Dryden, H. L. 1936 Air flow in the boundary layer near a plate. *NACA Rep.* 562.

Goldstein, M. E. 1994 Nonlinear interactions between oblique instability waves on nearly parallel shear flows. *Phys. Fluids* **6**, 724–735.

Goldstein, M. E. & Choi, S.-W. 1989 Nonlinear evolution of interacting oblique waves on two-dimensional shear layers. *J. Fluid Mech.* **207**, 97–120, and Corrigendum, **216**, 1990, 659–663.

Goldstein, M. E. & Durbin, P. A. 1986 Nonlinear critical layers eliminate the upper branch of spatially growing Tollmien-Schlichting waves. *Phys. Fluids* **29**, 2334–2345.

Goldstein, M. E., Leib, S. J. & Cowley, S. J. 1992 Distortion of a flat-plate boundary layer by free stream vorticity normal to the plate. *J. Fluid Mech.* **237**, 231–260.

Goldstein, M. E. & Wundrow, D. W. 1995 Interaction of oblique instability waves with weak streamwise vortices. *J. Fluid. Mech.* **284**, 377–407.

Hall, P. & Horseman, N. J. 1991 The linear inviscid secondary instability of longitudinal vortex structures in boundary layers. *J. Fluid Mech.* **232**, 357–375.

Hall, P. & Latkin, W. D. 1988 The fully nonlinear development of Görtler vortices in growing boundary layer. *Proc. R. Soc. Lond.* A **415**, 421–444.

Hall, P. & Seddougui, S. 1989 On the onset of three-dimensionality and time dependence in Görtler vortices. *J. Fluid Mech.* **204**, 405–420.

Hamilton, J. & Abernathy, F. 1994 Streamwise vortices and transition to turbulence. *J. Fluid Mech.* **264**, 185–212.

Kendall, J. M. 1985 Experimental study of disturbances produced in pre-transitional laminar boundary layer by weak free stream turbulence. *AIAA Paper* 85–1695.

Klebanoff, P. S. 1971 Effect of free-stream turbulence on a laminar boundary layer. *Bull. Am. Phys. Soc.* **10**, 1323.

Kogan, M. N., Shumilkin, V. G., Ustinov, M. V. & Zhigulev, S. V. 2001 Response of boundary layer flow to vortices normal to the leading edge. *Eur. J. Mech.* B *Fluids* **20**, 813–820.

Lighthill, M. J. 1957 The fundamental solution for small steady three-dimensional disturbances to a two-dimensional parallel shear flow. *J. Fluid Mech.* **3**, 113–14.

Matsubara, M. & Alfredsson, P. H. 2001 Disturbance growth in boundary layers subjected to free-stream turbulence. *J. Fluid Mech.* **430**, 149–168.

Nayfeh, A. H. 1981 Effect of streamwise vortices on Tollmien-Schlichting waves. *J. Fluid Mech.* **107**, 441–453.

Nayfeh, A. H. & Al-MaAitah, A. 1988 Influence of streamwise vortices on Tollmien-Schlichting waves. *Phys. Fluids* **31**, 3543–3549.

Roach, P. E. & Brierley, D. H. 1992 The influence of a turbulent free stream on zero pressure gradient transitional boundary layer development. Part I: Test cases T3A an T3B. In *Numerical Simulation of Unsteady Flows and Transition to Turbulence* (ed. P. Pironneau *et al.*), pp. 319–349. Cambridge University Press.

Taylor, G. I. 1939 Some recent developments in the study of turbulence. In *Proc. Fifth Int. Congr. for Applied Mechanics* (ed. J. P. Den Hartog & H. Peters), pp. 294–310. Wiley.

Ustinov, M. V. 2001 Response of the boundary layer developing over a blunt-nosed flat plate to free-stream non-uniformities. *Eur. J. Mech.* B *Fluids* **20**, 799–812.

Westin, K. J., Boiko, A. V., Klingmann, B. G. B., Kozlov, V. V. & Alfredsson, P. H. 1994 Experiments in a boundary layer subjected to free stream turbulence. Part 1. Boundary layer structure and receptivity. *J. Fluid Mech.* **281**, 193–218.

Wu, X. 1993 Nonlinear temporal-spatial modulation of near-planar Rayleigh waves in shear flows: formation of streamwise vortices. *J. Fluid Mech.* **256**, 685–719.

Wu, X. & Choudhari, M. 2003 Linear and nonlinear instabilities of a Blasius boundary layer perturbed by streamwise vortices. Part 2. Intermittent instability induced by long-wavelength Klebanoff modes. *J. Fluid Mech.* **483**, 249–286.

Wu, X., Lee, S. S. & Cowley, S. J. 1993 On the weakly nonlinear three-dimensional instability of shear flows to pairs of oblique waves: the Stokes layer as a paradigm. *J. Fluid Mech.* **253**, 681–721.

Wu, X., Stewart, P. A. & Cowley, S. J. 1996 On the weakly nonlinear development of Tollmien-Schlichting wave-trains in boundary layers. *J. Fluid Mech.* **316**, 133–171.